Zuschriften

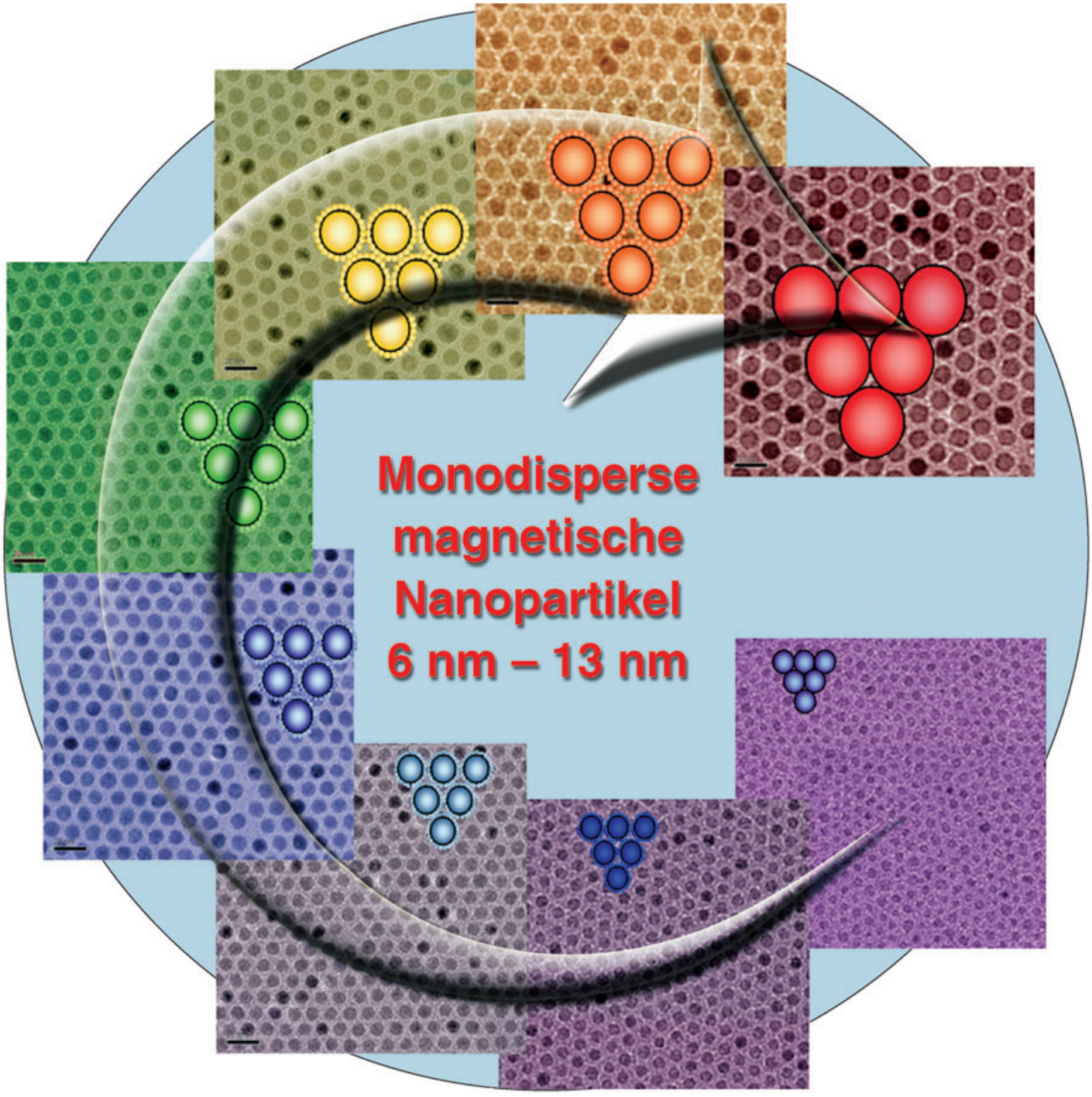

Monodisperse magnetische Eisenoxid-Nanopartikel mit einer kontinuierlichen Größenverteilung zwischen 6 und 13 nm wurden aus zuvor synthetisierten monodispersen Nanopartikel-Impflingen erhalten. Einzelheiten zur Synthese und Charakterisierung finden Sie in der Zuschrift von T. Hyeon et al. auf den folgenden Seiten.

  DOI: 10.1002/ange.200461665

Nanoparticle Synthesis

One-Nanometer-Scale Size-Controlled Synthesis of Monodisperse Magnetic Iron Oxide Nanoparticles**

*Jongnam Park, Eunwoong Lee, Nong-Moon Hwang, Misun Kang, Sung Chul Kim, Yosun Hwang, Je-Geun Park, Han-Jin Noh, Jae-Young Kim, Jae-Hoon Park, and Taeghwan Hyeon**

The synthesis of nanoparticles has been intensively pursued not only for their fundamental scientific interest but also for many technological applications,[1] monodisperse nanoparticles (standard deviations $\sigma \leq 5\%$) with controlled particle sizes are of key importance because the electrical, optical, and magnetic properties of these nanoparticles depend strongly on their size.[2,3]

Recently, several colloidal chemical synthetic procedures have been developed to produce monodisperse nanoparticles of various materials. In the classical LaMer mechanism, a short burst of nucleation from a supersaturated solution is followed by the slow growth of particles without any significant additional nucleation, thereby achieving a complete separation of nucleation and growth.[4] Various similar procedures have been employed to synthesize almost monodisperse nanoparticles of CdSe,[5] related II–VI semiconductors,[5] and magnetic materials.[6] Watzky and Finke introduced a novel synthetic procedure that combines slow, continuous nucleation and fast, autocatalytic surface growth.[7] More recently, seed-mediated growth has been employed for the synthesis of larger metallic nanoparticles on smaller seeds. For example, Buhro and co-workers reported the synthesis of monodisperse nanoparticles of Bi, Sn, and In using Au nanoclusters as seeds.[8] In addition, monodisperse nanoparticles of Au,[9] Fe,[10] and Fe_3O_4[11] have been synthesized following similar procedures. Many monodisperse gold nanoparticles have been synthesized by a digestive ripening process or by surfactant exchange reactions.[12] The ultimate goal in the synthesis of nanoparticles is atomic-level size-controlled synthesis, similar to atomic layer deposition in thin-film processing,[13] of monodisperse nanoparticles without a size-selection process (Scheme 1), which has yet to be achieved.

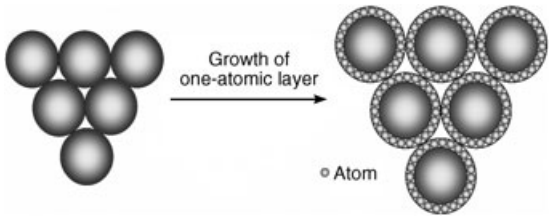

Scheme 1. Direct and atomic-scale controlled synthesis of monodisperse nanoparticles.

Our research group has developed new procedures for the synthesis of monodisperse nanocrystals of metals,[1e,4] metal oxides,[15] and metal sulfides[16] without going through a laborious size-sorting process. In these syntheses, metal–surfactant complexes generated in situ are thermally decomposed to form monodisperse nanoparticles. We report herein the synthesis of monodisperse iron oxide nanoparticles with a continuous size spectrum of 6–13 nm.

The process conditions required for the synthesis of monodisperse particles of micrometer size are relatively well established,[17] and a similar principle is expected to apply to the synthesis of monodisperse nanoparticles. It would be ideal if a certain species contributes exclusively to growth, instead of participating in both nucleation and growth processes, which means that the growth process is separated from additional nucleation. Such a separation between nucleation and growth is necessary for the direct synthesis of monodisperse nanoparticles, and this condition must have been satisfied in our previous direct synthesis of monodisperse iron nanoparticles.[1e,15a] On analyzing these procedures,[1e,15a] we tried to distinguish the species that contributes to nucleation from that which contributes to growth and reached a conclusion that pentacarbonyliron mainly contributes to nucleation, whereas the iron oleate complex generated in situ contributes exclusively to growth. We also found that the nucleation resulting from the thermal decomposition of pentacarbonyliron takes place at relatively low temperature, whereas the growth derived from the decomposition of the iron oleate complex occurs at a higher temperature. In other

[*] J. Park, E. Lee, S. C. Kim, Prof. Dr. T. Hyeon
National Creative Research Initiative Center for Oxide Nanocrystalline Materials and
School of Chemical and Biological Engineering
Seoul National University
Seoul 151-744 (Korea)
Fax: (+82) 2-886-8457
E-mail: thyeon@plaza.snu.ac.kr
Prof. Dr. N.-M. Hwang
School of Materials Science and Engineering and
Nano-Systems Institute (NSI-NCRC)
Seoul National University
Seoul 151-744 (Korea)
M. Kang, Y. Hwang, Prof. Dr. J.-G. Park
Department of Physics and Institute of Basic Science
Sungkyunkwan University, Suwon 440-746 (Korea)
Dr. H.-J. Noh, Dr. J.-Y. Kim, Prof. Dr. J.-H. Park
Department of Physics and
Pohang Light Source
Pohang University of Science and Technology
Pohang 790-784 (Korea)

[**] T.H. thanks the National Creative Research Initiative Program of the Korean Ministry of Science and Technology for financial support. N.M.H. thanks the National Core Research Center program of the Korea Science and Engineering Foundation (KOSEF) through the NANO systems Institute at Seoul National University for support. The work at POSTECH was supported by KISTEP through the X-ray/particle-beam Nanocharacterization Program. The work at Sungkyunkwan University was supported by the CSCMR and the Proton Accelerator User Program (No. M102KS010001-02K1901-01810) of the Proton Engineering R&D Project.

Supporting information for this article is available on the WWW under http://www.angewandte.org or from the author.

words, nucleation and growth seem to be ideally separated in our procedure. Consequently, we reasoned that if we prepare the iron oleate complex separately and use the complex as a growth source, we might synthesize monodisperse iron nanoparticles with controlled size by the additional incremental growth of the previously synthesized monodisperse iron nanoparticles. The overall process is similar to seed-mediated growth.[8–11]

As we described previously, we were able to synthesize monodisperse iron nanoparticles with sizes of 4, 8, and 11 nm from reaction mixtures containing 1:1, 1:2, and 1:3 molar ratios of pentacarbonyliron and oleic acid, respectively. Solutions containing 1.5, 3.0, and 4.5 mmol of the iron oleate complex were prepared by heating appropriate amounts of pentacarbonyliron and oleic acid in dioctyl ether at 403 K for 12 h. After refluxing the mixtures generated from the various combinations of the iron nanoparticles and the iron oleate solutions, we were able to synthesize monodisperse iron nanoparticles with particle sizes of 6, 7, 9, 10, 12, 13, and 15 nm (Table 1).

Table 1: Size of final iron nanoparticles produced from combinations of initial monodisperse iron nanoparticles and iron oleate solutions.

Final iron nanoparticles [nm]	Initial iron nanoparticles [nm]	Iron oleate solution [mmol]
6	4	1.5
7	4	3.0
9	8	1.5
10	8	3.0
12	11	1.5
13	11	3.0
15	11	4.5

These iron nanoparticles were readily oxidized to iron oxide on exposure to air.[18] The transmission electron microscopy (TEM) images of the air-oxidized iron oxide nanoparticles are shown in Figure 1. All of the nanoparticles, except the 6-nm-sized particles ($\sigma = 8.5\,\%$), exhibit particle-size distributions with standard deviations (σ) of less than 5%. These monodisperse nanoparticles were obtained directly without a size-selection process, and the synthetic procedure is highly reproducible. We expect that this concept of continuous growth without additional nucleation should be applicable to the incremental 1-nm size-controlled synthesis of monodisperse nanoparticles of many other materials. Subsequent further oxidation of these nanoparticles with trimethylamine *N*-oxide produced monodisperse and highly crystalline iron oxide nanocrystals. The TEM images of the resulting chemically oxidized nanocrystals are very similar to those obtained before the chemical oxidation in terms of particle sizes and their distributions, and the high-resolution transmission electron microscopy (HRTEM) images reveal their highly crystalline nature (see the Supporting Information).

The iron oxide nanocrystals were characterized by X-ray powder diffraction (XRD), X-ray absorption spectroscopy (XAS), and X-ray magnetic circular dichroism (XMCD). The XAS and XMCD measurements were performed at Pohang Light Source 2A1 beamline. The XRD patterns of the nanocrystals (Figure 2a) were assigned to the (111), (220), (311), (400), (422), (511), and (440) reflections of the inverse spinel structure of maghemite (γ-Fe_2O_3; JCPDS no. 39–1346). It should be noted that the standard XRD patterns of magnetite (Fe_3O_4) and maghemite are nearly identical. As the particle sizes get larger, the XRD peaks become narrower (Figure 2b), and the particle sizes calculated from the Scherrer formula match well with those obtained from the TEM data (see the Supporting Information).

X-ray absorption spectroscopy (XAS) and X-ray magnetic circular dichroism (XMCD) measurements at the Fe $L_{2,3}$ edges were carried out for the quantitative identification of the compositions of the iron oxide nanocrystals. Figure 3a, b show the XAS spectra and XMCD results, respectively, of the iron oxide nanocrystals with diameters of 4, 6, 8, 9, 11, and 13 nm, in comparison with those of two reference materials, bulk γ-Fe_2O_3 (maghemite) and bulk Fe_3O_4 (magnetite), which have nearly the same spinel crystal structure with only about 1% difference in the cubic lattice constant. Both the XAS and MCD spectra of the 4-nm-sized nanocrystals are very similar to those of γ-Fe_2O_3, which contains only a Fe^{3+} ion. As the particle size increases, the line shapes gradually change and both spectra for the iron oxide nanocrystals with a large particle size became similar to those of Fe_3O_4, which contains Fe^{3+} and Fe^{2+} ions. From the XAS and XMCD results, we were able to make a quantitative estimation of the compositions of the iron oxide nanocrystals in the form of $(\gamma\text{-}Fe_2O_3)_{1-x}(Fe_3O_4)_x$. The estimations are $x = 0.20 \pm 0.05$, 0.35 ± 0.05, 0.44 ± 0.05, 0.52 ± 0.05, 0.62 ± 0.05, 0.64 ± 0.05, and 0.65 ± 0.05 for the 4-, 6-, 8-, 9-, 11-, 12-, and 13-nm-sized nanocrystals, respectively. Therefore, γ-Fe_2O_3 is the dominant phase of the small 4-nm-sized iron oxide nanocrystals, whereas the fraction of the Fe_3O_4 component gradually increases with increasing particle size.

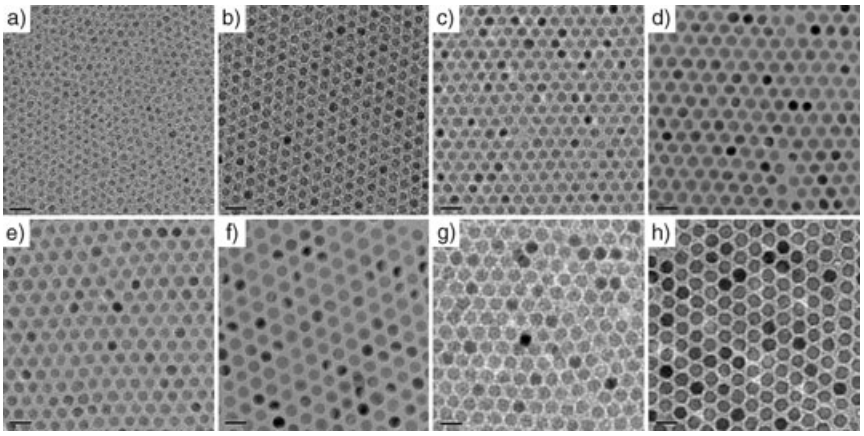

Figure 1. TEM images of a) 6-, b) 7-, c) 8-, d) 9-, e) 10-, f) 11-, g) 12-, and h) 13-nm-sized air-oxidized iron oxide nanoparticles showing the one nanometer level increments in diameter. (The enlarged TEM images and particle-size distribution histograms are supplied in the Supporting Information.)

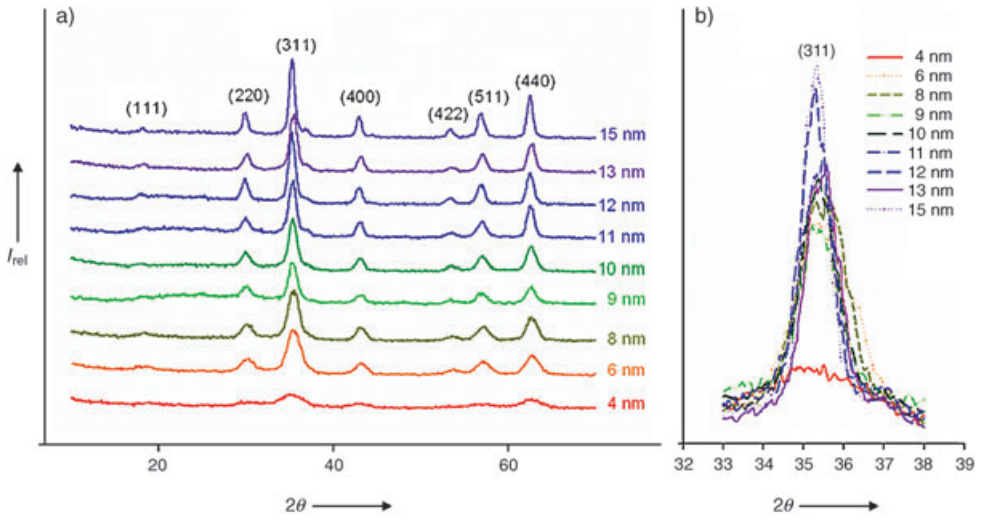

Figure 2. a) XRD patterns of iron oxide nanocrystals of 4, 6, 8, 9, 10, 11, 12, 13, and 15 nm, and b) the change of the (311) peak intensity of each nanocrystal.

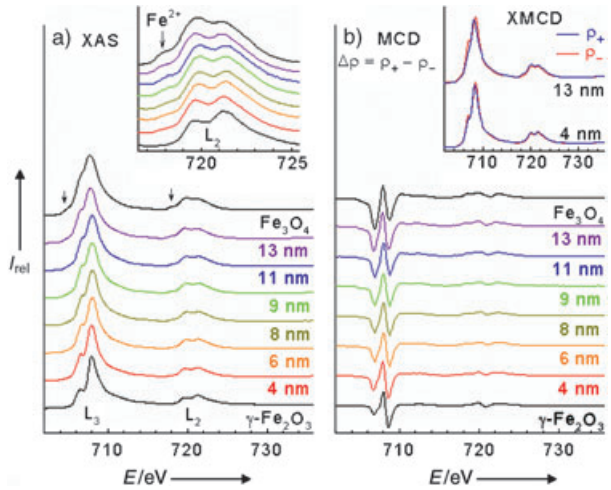

Figure 3. Fe $L_{2,3}$ edge a) XAS and b) XMCD spectra of 4, 6, 8, 9, 11, and 13 nm iron oxide nanocrystals compared with those of bulk reference materials (γ-Fe_2O_3 and Fe_3O_4). The magnified L_2 region XAS spectra of the nanocrystals and XMCD spectra of the 4 and 13 nm nanocrystals are shown in the insets of (a) and (b), respectively.

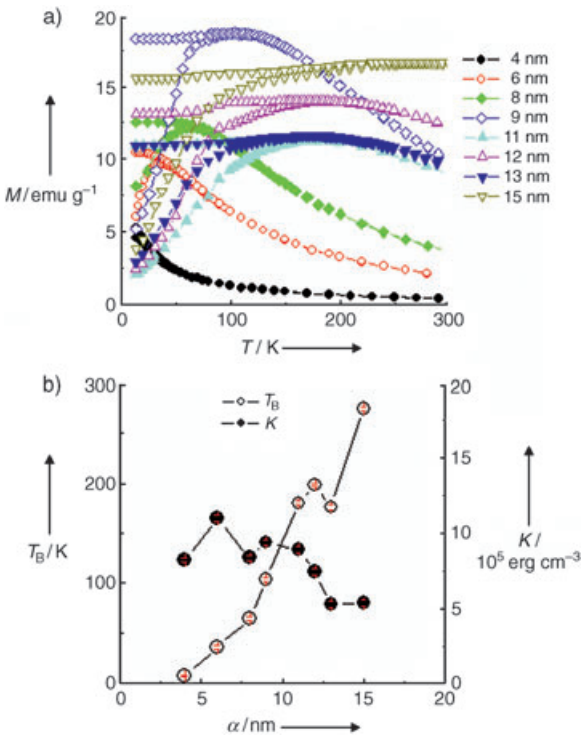

Figure 4. a) Temperature dependence of magnetization measured after zero-field cooling (ZFC) and field cooling (FC) at 100 Oe for 4, 6, 8, 9, 11, 12, 13, and 15 nm particles. b) Size dependence of the blocking temperature, T_B, obtained from M(*T*) in Figure 4a. The magnetic anisotropy constant, *K*, was obtained as described in the text.

The magnetic properties of these iron oxide nanocrystals were studied using a vibrating sample magnetometer (Lake Shore, 9300). Figure 4a shows the temperature dependence of magnetization measured at 100 Oe from 300 to 14 K. All our samples show superparamagnetic behavior at high temperatures. However, on cooling, the zero-field-cooled magnetization begins to drop and deviate from the field-cooled magnetization at the blocking temperature T_B. For the 4 nm sample, the blocking temperature seems to be close to the lowest temperature measured (14 K). For further measurements of the magnetization down to 2 K, we used a SQUID magnetometer and found that the blocking temperature is 8 K. With increasing particle size, the blocking temperature increases continuously (Figure 4b); for example, the blocking temperature increases to 275 K for the 15-nm-sized nanocrystals. We then used the measured blocking temperature to calculate the magnetic anisotropy constant K by using the formula: $K = 25 k_B T_B V^{-1}$,[19] where k_B is the Boltzman constant, T_B is the measured blocking temperature, and V is the total volume of a particle whose diameter was determined from TEM measurements. Considering that all our samples are spherical and, consequently, there is no shape anisotropy involved for the nanocrystals, the dominant anisotropy should be because of magnetocrystalline anisotropy. It is noticeable

that, unlike other nanocrystals, the magnetic anisotropy constant does not increase significantly with a reduction in particle size. For comparison, the magnetic anisotropy constant[20] of bulk Fe_3O_4 is $4\times10^5\,erg\,cm^{-3}$, which is slightly higher than that of our 15-nm-sized sample. This unusual result seems to be because of the strong dipolar interactions between the nanoparticles, which might mask the size dependence of the magnetic anisotropy. In fact, the peaks in the magnetic susceptibility appear to be much broader than would be expected for monodisperse nanoparticles, thus demonstrating the strong dipolar interaction in our samples.

In conclusion, we have synthesized monodisperse iron oxide nanoparticles with a continuous size spectrum of 6–13 nm. The synthesis of iron nanoparticles with particle sizes of 6, 7, 9, 10, 12, 13, and 15 nm was achieved by the controlled additional growth of the previously synthesized monodisperse iron nanoparticles; the overall synthetic procedure is similar to seed-mediated growth. These monodisperse nanoparticles were obtained directly without a size-selection process, and the synthetic procedure is highly reproducible. Subsequent chemical oxidation produced monodisperse and highly crystalline iron oxide nanocrystals. This concept of continuous growth without additional nucleation could be applicable to other materials for the incremental, 1-nm size-controlled synthesis of monodisperse nanoparticles.

Experimental Section

Monodisperse 4-, 8-, and 11-nm-sized iron oxide nanoparticles were prepared as described previously.[15a] For example, to prepare 11-nm-sized monodisperse iron nanoparticles, $[Fe(CO)_5]$ (0.2 mL, 1.52 mmol; Aldrich, 99.999%) was added to a mixture containing dioctyl ether (10 mL; Aldrich, 90%), and oleic acid (1.28 g, 4.56 mmol; Aldrich, 99%) at 373 K. The resulting mixture was heated to reflux and kept at that temperature for 1 h. During this process, the initial orange solution gradually became black. It was then cooled to room temperature and anhydrous trimethylamine *N*-oxide (0.34 g, 4.56 mmol, prepared from $(CH_3)_3NO{\cdot}2H_2O$: Aldrich, 98%) was added. The mixture was then heated to 403 K in an argon atmosphere and maintained at this temperature for 2 h, whereupon the solution became brown. The reaction temperature was slowly increased to reflux and the reflux continued for 1 h; the color of the solution gradually turned from brown to black. The solution was then cooled to room temperature, and ethanol was added to yield a black precipitate, which was then separated by centrifugation. Starting mixtures containing $[Fe(CO)_5]$ and oleic acid in 1:1 and 1:2 molar ratios yielded iron oxide nanoparticles of 4 and 8 nm, respectively.

Iron oleate complex solutions with three different concentrations were prepared by mixing $[Fe(CO)_5]$ (0.2 mL, 1.52 mmol), dioctyl ether (10 mL), and oleic acid (0.43 g, 1.52 mmol; 0.85 g, 3.04 mmol; or 1.28 g, 4.56 mmol; respectively) which were heated at 403 K for 12 h to form the iron oleate complex solutions designated as 1.5, 3.0, and 4.5 mmol, respectively. For the synthesis of iron nanoparticles of the desired sizes, various combinations of the iron oleate solutions and the iron nanoparticle suspensions (before the chemical oxidation with trimethylamine *N*-oxide) were mixed (Table 1). The resulting solution was heated to reflux for 1 h to produce iron nanoparticles that were further oxidized with anhydrous trimethylamine *N*-oxide to produce highly crystalline iron oxide nanocrystals.

Received: August 16, 2004
Revised: February 2, 2005
Published online: March 30, 2005

Keywords: iron · magnetic properties · materials science · nanoparticles

[1] a) G. Schmid, *Nanoparticles: From Theory to Application*, Wiley-VCH, Weinheim, **2004**; b) K. J. Klabunde, *Nanoscale Materials in Chemistry*, Wiley-Interscience, New York, **2001**; c) A. P. Alivisatos, *Science* **1996**, *271*, 933; d) C. Pacholski, A. Kornowsli, H. Weller, *Angew. Chem.* **2002**, *114*, 1234; *Angew. Chem. Int. Ed.* **2002**, *41*, 1188; e) T. Hyeon, *Chem. Commun.* **2003**, 927; f) M. P. Pileni, *Nat. Mater.* **2003**, *2*, 145.

[2] a) M. Nirmal, L. Brus, *Acc. Chem. Res.* **1999**, *32*, 407; b) C. B. Murray, C. R. Kagan, M. G. Bawendi, *Annu. Rev. Mater. Sci.* **2000**, *30*, 545; c) A. L. Rogach, D. V. Talapin, E. V. Shevchenko, A. Kornowski, M. Haase, H. Weller, *Adv. Funct. Mater.* **2002**, *12*, 653.

[3] a) S. Sun, C. B. Murray, D. Weller, L. Folks, A. Moser, *Science* **2000**, *287*, 1989; b) D. E. Speliotis, *J. Magn. Magn. Mater.* **1999**, *193*, 29; c) R. C. O'Handley, *Modern Magnetic Materials*, Wiley, New York, **1999**.

[4] V. K. LaMer, R. H. Dinegar, *J. Am. Chem. Soc.* **1950**, *72*, 4847.

[5] a) C. B. Murray, D. J. Norris, M. G. Bawendi, *J. Am. Chem. Soc.* **1993**, *115*, 8706; b) X. Peng, J. Wickham, A. P. Alivisatos, *J. Am. Chem. Soc.* **1998**, *120*, 5343; c) D. V. Talapin, A. L. Rogach, E. V. Shevchenko, A. Kornowski, M. Haase, H. Weller, *J. Am. Chem. Soc.* **2002**, *124*, 5782; d) Z. A. Peng, X. Peng, *J. Am. Chem. Soc.* **2001**, *123*, 183; e) W. W. Yu, X. Peng, *Angew. Chem.* **2002**, *114*, 2474; *Angew. Chem. Int. Ed.* **2002**, *41*, 2368.

[6] a) S. Sun, C. B. Murray, *J. Appl. Phys.* **1999**, *85*, 4325; b) F. Dumestre, B. Chaudret, C. Amiens, P. Renaud, P. Fejes, *Science* **2004**, *303*, 821; c) E. V. Shevchenko, D. V. Talapin, A. L. Rogach, A. Kornowski, M. Haase, H. Weller, *J. Am. Chem. Soc.* **2002**, *124*, 11480; d) F. Dumestre, B. Chaudret, C. Amiens, M. Respaud, P. Fejes, P. Renaud, P. Zurcher, *Angew. Chem.* **2003**, *115*, 5371; *Angew. Chem. Int. Ed.* **2003**, *42*, 5213; e) F. Dumestre, B. Chaudret, C. Amiens, M.-C. Fromen, M.-J. Casanove, M. Respaud, P. Zurcher, *Angew. Chem.* **2002**, *114*, 4462; *Angew. Chem. Int. Ed.* **2002**, *41*, 4286; f) J. Park, B. Koo, Y. Hwang, C. Bae, K. An, J.-G. Park, H. M. Park, T. Hyeon, *Angew. Chem.* **2004**, *116*, 2332; *Angew. Chem. Int. Ed.* **2004**, *43*, 2282; g) V. F. Puntes, K. M. Krishnan, A. P. Alivisatos, *Science* **2001**, *291*, 2115; h) V. F. Puntes, D. Zanchet, C. K. Erdonmez, A. P. Alivisatos, *J. Am. Chem. Soc.* **2002**, *124*, 12874; i) S.-J. Park, S. Kim, S. Lee, Z. G. Khim, K. Char, T. Hyeon, *J. Am. Chem. Soc.* **2000**, *122*, 8581.

[7] a) M. A. Watzky, R. G. Finke, *J. Am. Chem. Soc.* **1997**, *119*, 10382; b) K. R. Brown, M. J. Natan, *Langmuir* **1998**, *14*, 726.

[8] H. Yu, P. C. Gibbons, K. F. Kelton, W. E. Buhro, *J. Am. Chem. Soc.* **2001**, *123*, 9198.

[9] a) N. R. Jana, X. Peng, *J. Am. Chem. Soc.* **2003**, *125*, 14280; b) J. P. Wilcoxon, P. P. Provencio, *J. Am. Chem. Soc.* **2004**, *126*, 6402.

[10] D. Farrell, S. A. Majetich, J. P. Wilcoxon, *J. Phys. Chem. B* **2003**, *107*, 11022.

[11] a) S. Sun, H. J. Zeng, *J. Am. Chem. Soc.* **2002**, *124*, 8204; b) S. Sun, H. Zeng, D. B. Robinson, S. Raoux, P. M. Rice, S. X. Wang, G. Li, *J. Am. Chem. Soc.* **2004**, *126*, 273.

[12] a) X. M. Lin, H. M. Jaeger, C. M. Sorensen, K. J. Klabunde, *J. Phys. Chem. B* **2001**, *105*, 3353; b) S. Stoeva, K. J. Klabunde, C. M. Sorensen, I. Dragieva, *J. Am. Chem. Soc.* **2002**, *124*, 2305; c) B. L. V. Prasad, S. I. Stoeva, C. M. Sorensen, K. J. Klabunde, *Chem. Mater.* **2003**, *15*, 935; d) S. I. Stoeva, B. L. V. Prasad, S. Uma, P. K. Stoimenov, V. Zaikovski, C. M. Sorensen, K. J. Klabunde, *J. Phys. Chem. B* **2003**, *107*, 7441; e) T. Shimizu, T. Teranishi, S. Hasegawa, M. Miyake, *J. Phys. Chem. B* **2003**, *107*, 2719; f) T. Teranishi, S. Hasegawa, T. Shimizu, M. Miyake, *Adv. Mater.* **2001**, *13*, 1699; g) L. O. Brown, J. E. Hutchison, *J. Phys.*

Chem. B **2001**, *105*, 8911; h) L. O. Brown, J. E. Hutchison, *J. Am. Chem. Soc.* **1999**, *121*, 882; i) J. E. Martin, J. P. Wilcoxon, J. Odinek, P. Provencio, *J. Phys. Chem. B* **2000**, *104*, 9475.

[13] M. Leskela, M. Ritala, *Angew. Chem.* **2003**, *115*, 5706; *Angew. Chem. Int. Ed.* **2003**, *42*, 5548.

[14] a) S.-W. Kim, J. Park, Y. Jang, Y. Chung, S. Hwang, T. Hyeon, Y. W. Kim, *Nano Lett.* **2003**, *3*, 1289; b) S. U. Son, Y. Jang, J. Park, H. B. Na, H. M. Park, H. J. Yun, J. Lee, T. Hyeon, *J. Am. Chem. Soc.* **2004**, *126*, 5026; c) S. U. Son, I. K. Park, J. Park, T. Hyeon, *Chem. Commun.* **2004**, 778.

[15] a) T. Hyeon, S. S. Lee, J. Park, Y. Chung, H. B. Na, *J. Am. Chem. Soc.* **2001**, *123*, 12798; b) T. Hyeon, Y. Chung, J. Park, S. S. Lee, Y.-W. Kim, B. H. Park, *J. Phys. Chem. B* **2002**, *106*, 6831; c) J. Park, K. An, Y. Hwang, J.-G. Park, H.-J. Noh, J.-Y. Kim, J.-H. Park, N.-M. Hwang, T. Hyeon, *Nat. Mater.* **2004**, *3*, 891; d) J. Joo, T. Yu, Y.-W. Kim, H. M. Park, F. Wu, J. Z. Zhang, T. Hyeon, *J. Am. Chem. Soc.* **2003**, *125*, 6553.

[16] J. Joo, H. B. Na, T. Yu, J. H. Yu, Y.-W. Kim, F. Wu, J. Z. Zhang, T. Hyeon, *J. Am. Chem. Soc.* **2003**, *125*, 11100.

[17] a) T. Sugimoto, *Monodispersed Particles*, Elsevier, Amsterdam, **2001**; b) T. Sugimoto, *Adv. Colloid Interface Sci.* **1987**, *28*, 65.

[18] K. Woo, J. Hong, S. Choi, H.-W. Lee, J.-P. Ahn, C. S. Kim, S. W. Lee, *Chem. Mater.* **2004**, *16*, 2814.

[19] B. D. Cullity, *Introduction to Magnetic Materials*, Addison-Wiley, Reading, **1972**.

[20] S. Chikazumi, *Physics of Ferromagnetism*, 2nd ed., Clarendon, Oxford, **1997**.

